Journal of Controlled Release 293 (2019) 10–20

Contents lists available at ScienceDirect

Journal of Controlled Release

journal homepage: www.elsevier.com/locate/jconrel

Controlled release strategy designed for intravitreal protein delivery to the retina

Vianney Delplace[a], Arturo Ortin-Martinez[b], En Leh S. Tsai[b], Alan N. Amin[a], Valerie Wallace[b,c,d], Molly S. Shoichet[a,e,*]

[a] Chemical Engineering & Applied Chemistry, University of Toronto, 200 College Street, Toronto, ON M5S 3E5, Canada
[b] Donald K. Johnson Eye Institute, Krembil Research Institute, University Health Network, Toronto, ON M5T 2S8, Canada
[c] Department of Laboratory Medicine and Pathobiology, University of Toronto, 27 King's College Circle, Toronto, ON M5S 1A1, Canada
[d] Department of Ophthalmology and Vision Sciences, University of Toronto, 340 College Street, Toronto, ON M5T 3A9, Canada
[e] Institute of Biomaterials & Biomedical Engineering, University of Toronto, 164 College Street, Toronto, ON M5S 3G9, Canada

ARTICLE INFO

Keywords:
Ocular delivery
Hydrogel
Affinity release
Mathematical model
Drug delivery

ABSTRACT

Therapeutic protein delivery directly to the eye is a promising strategy to treat retinal degeneration; yet, the high risks of local drug overdose and cataracts associated with bolus injection have limited progress, requiring the development of sustained protein delivery strategies. Since the vitreous humor itself is a gel, hydrogel-based release systems are a sensible solution for sustained intravitreal protein delivery. Using ciliary neurotrophic factor (CNTF) as a model protein for ocular treatment, we investigated the use of an intravitreal, affinity-based release system for protein delivery. To sustain CNTF release, we took advantage of the affinity between Src homology 3 (SH3) and its peptide binding partners: CNTF was expressed as a fusion protein with SH3, and a thermogel of hyaluronan and methylcellulose (HAMC) was modified with SH3 binding peptides. Using a mathematical model, the hydrogel composition was successfully designed to release CNTF-SH3 over 7 days. The stability and bioactivity of the released protein were similar to those of commercial CNTF. Intravitreal injections of the bioengineered thermogel showed successful delivery of CNTF-SH3 to the mouse retina, with expected transient downregulation of phototransduction genes (e.g., rhodopsin, S-opsin, M-opsin, Gnat 1 and 2), upregulation of STAT1 and STAT3 expression, and upregulation of STAT3 phosphorylation. This constitutes the first demonstration of intravitreal protein release from a hydrogel. Immunohistochemical analysis of the retinal tissues of injected eyes confirmed the biocompatibility of the delivery vehicle, paving the way towards new intravitreal protein delivery strategies.

1. Introduction

Therapeutic protein delivery to the retina is promising for the treatment of prevalent degenerative diseases. Age-related macular degeneration, diabetic retinopathy and retinitis pigmentosa (RP) are among the retinal conditions shown to benefit from innovative protein-based treatments pre-clinically [1–4]. Yet, ocular delivery of proteins is challenging. Eye drops are rapidly cleared, thereby limiting the benefits of topical application, and the blood-retinal barrier at the back of the eye reduces the efficacy of systemic administration [5]. Thus, repeated bolus intravitreal injections remain the standard route of administration, but have higher risks of drug overdose, inflammation (e.g., uveitis, endophthalmitis) and cataracts [6]. This challenge prompted us to investigate the use of a bioengineered intravitreal hydrogel for sustained, local therapeutic protein delivery to the retina, using ciliary neurotrophic factor (CNTF) for proof of concept.

CNTF has long been studied for its neuroprotective effect on the retina. In various degenerative animal models (e.g., mice, rats, dogs), CNTF consistently leads to prolonged photoreceptor cell survival and increased outer nuclear layer (ONL) thickness [7], intensifying interest for its sustained delivery. For example, CNTF-secreting retinal pigment epithelial cells encapsulated in an implantable device and placed in the vitreous, were shown to effectively release CNTF, with no adverse events in patients [8–10]. However, while this device is entering phase 3 clinical trials for the treatment of a rare retinal disease (macular telangiectasia) [11,12], long-term implantation showed no improvements in visual acuity in RP patients [13]. Moreover, such an implant requires a complex, invasive surgery, followed by implant removal, and

* Corresponding author at: Donnelly Centre, University of Toronto, 160 College Street, Toronto, ON M5S 3E1, Canada.
E-mail address: molly.shoichet@utoronto.ca (M.S. Shoichet).

https://doi.org/10.1016/j.jconrel.2018.11.012
Received 1 August 2018; Received in revised form 5 November 2018; Accepted 9 November 2018
Available online 10 November 2018
0168-3659/

the long-term fate of encapsulated cells remains a concern. These findings highlight the need for less invasive delivery approaches.

An intravitreal controlled release system should allow sustained delivery while being injectable through a fine-gauge needle for minimal invasiveness. Taking advantage of electrostatic or other non-covalent interactions, various strategies have been developed to locally sustain protein release for other applications [14]. Extracellular matrix components (e.g., heparin, fibrin) that naturally bind proteins [15–20] have been successfully applied for the tunable delivery of various growth factors, such as vascular endothelial growth factor (VEGF), platelet-derived growth factor-BB (PDGF-BB), and transforming growth factor-β1 (TGF-β1) [21]. More recently, hydrogel/particle composite materials have been explored, either using the competitive binding properties of nucleic acid aptamers to release factors on demand [22], or self-regulated electrostatic interactions from embedded, negatively-charged PLGA nanoparticles [23]. However, none of these strategies have been applied to intravitreal protein delivery to date. Intravitreal nanotherapies have been extensively studied for small molecule drugs [24–26], but the typical harsh encapsulation conditions often reduce their utility for protein delivery. Thus, only few examples of nanoparticle-mediated, intravitreal protein delivery systems have been reported, with limited success [27–29].

Given that the vitreous humor is a gel primarily composed of hyaluronan, we anticipated that hyaluronan-based hydrogels would be beneficial for intravitreal delivery when designed with the following characteristics: biocompatible, injectable or rapidly in-situ forming, bioresorbable or biodegradable, and transparent. In the context of intravitreal release, the anti-VEGF antibody, bevacizumab, was physically entrapped in either a synthetic thermogel of poly(2-ethyl-2-oxazoline)-b-poly(ε-caprolactone)-b-poly(2-ethyl-2-oxazoline) [30] or a crosslinked chitosan-alginate hydrogel [31], but its release was only evaluated in vitro. The safety of intravitreal injections of poly(ethylene glycol) diacrylate crosslinked poly(N-isopropylacrylamide) was assessed in mice, revealing a detrimental effect on retinal thickness and function [32]. These striking observations prompted us to develop a novel and safe approach for the delivery of growth factors to the retina.

We designed a hydrogel to provide sustained release of CNTF to the retina when injected in the vitreous humor (Fig. 1). The hydrogel is composed of a physical blend of hyaluronan (HA) and methylcellulose (MC), that we refer to as HAMC and which is an inverse thermogelling polymer [33–35]. To control the release of CNTF, it is recombinantly expressed as a fusion protein with the Src homology 3 (SH3) domain while HAMC is modified with an SH3 binding peptide with a dissociation constant (K_D) of approximately 10^{-5} M, thereby allowing reversible binding of the fusion protein to the gel matrix [36]. For the first time, the peptide-modified HAMC hydrogel was designed to achieve the desired affinity release using a previously-developed mathematical model [37]. Using this model, the SH3 binding peptide concentration can be predicted for a desired release profile, independent of the protein concentration and the protein-to-peptide ratio. The structure, stability, bioactivity and controlled release of CNTF-SH3 are investigated in vitro prior to evaluating intravitreal release and protein bioactivity from our hydrogel-based delivery system in the mouse eye.

2. Material and methods

2.1. Materials

pET24 vector was purchased from Invitrogen (Burlington, Canada). Restriction enzymes were purchased from New England Biolabs (Pickering, ON). Pharma grade high molecular weight sodium hyaluronate (HMW HA) (1.2–1.9 MDa) was purchased from NovaMatrix, and methylcellulose of 300 kg.mol^{-1} was purchased from Shin Etsu (Tokyo, Japan). Anti-CNTF antibody was purchased from Abcam (Cambridge, USA). All buffers were made with deionized water. All other solvents and reagents were purchased from Sigma-Aldrich and used as received. Static light scattering was measured using a UNit apparatus (Unchained Labs Inc.).

2.2. Protein expression

To obtain His–SH3–CNTF–FLAG DNA, a sequence coding for CNTF with a C-terminal FLAG tag was subcloned into a pET24d + vector already containing the sequence coding for His-SH3 followed by a flexible linker region. The flexible linker region was added to ensure that the activity of CNTF would not be affected by the addition of this extra bulk at the N-terminus, as had been previously demonstrated with another construct [38]. CNTF was inserted into this target vector using the restriction enzymes *Xho*I and *Eag*I. The plasmid was transformed into chemically competent BL21(DE3) *Escherichia coli* cells, plated on Luria-Bertani (LB)-agar plates containing 50 μg mL^{-1} kanamycin and incubated overnight at 37 °C. Resulting clones were grown in starter cultures of 20 mL of Luria-Bertani (LB) broth containing 50 μg mL^{-1} kanamycin overnight at 37 °C. Starter cultures were inoculated into 1.8 L of Terrific Broth (TB) supplemented with 0.8% glycerol, 50 μg mL^{-1} kanamycin, and 5 drops of Anti-foam 204. Cells were grown at 37 °C, with air sparging, until an OD600 of 0.8–1.0 was reached (approximately 2 h). Cells were then induced with a final concentration of 0.8 mM IPTG and grown overnight at 16 °C, with 5 additional drops of antifoaming agent. Cells were pelleted by centrifugation for 10 min at 7000 rpm and 4 °C (Beckman Coulter centrifuge Avanti J-26 with rotor JLA-8.1000). Cell pellets were transferred to 50-mL falcon tubes, and re-suspended in 30 mL of binding buffer (50 mM Tris pH 7.5, 500 mM NaCl, 5 mM imidazole), prior to sonication for 5 min at 30% amplitude with a pulse of 2 s (Misonix S-4000 Sonicator Ultrasonic Processor equipped with a Dual Horn probe). The slurry was centrifuged at 45,000 *g* for 15 min at 4 °C (Beckman Coulter centrifuge Avanti J-26 with rotor JA-25.50). The liquid fraction was incubated with 1 mL of Ni-NTA resin solution for 15 min at 4 °C. The resin was collected in a column with a glass frit, washed 10 × 10 mL with wash buffer (50 mM Tris, pH 7.5, 500 mM NaCl, 30 mM imidazole), and eluted with 5 × 5 mL elution buffer (50 mM Tris, pH 7.5, 500 M NaCl, 250 mM imidazole). From a Bradford assay, the elution fractions containing the expressed protein were combined and dialyzed against PBS overnight. The eluate was then concentrated to 3 mL using a Vivaspin centrifugal filter (MWCO 10 kDa; Sartorius), filtered and further purified by fast protein liquid chromatography (FPLC) (FPLC, Hi-load 16/60 Superdex 200 prep grade column, AKTA Explorer 10, Amersham Pharmacia) in PBS. Protein concentrations were determined by absorbance at 280 nm using an ND-1000 Nanodrop spectrophotometer. The protein was analyzed by SDS-PAGE and mass spectrometry, and concentrated before long-term storage at −80 °C.

2.3. MC-peptide synthesis

Maleimide-modified SH3-binding peptide (sequence: GGGKPPVV-KKPHYLS) was synthesized as previously reported [36]. MC-peptide was synthesized using a previously reported method, with some modifications described here [36,39]. Unless specified, all reactions and dialyses were carried out at 4 °C. MC was carboxylated using a Williamson ether synthesis (10 equivalents of bromoacetic acid), and purified by dialysis. Carboxylated MC was activated with 3 equivalents of (4-(4,6-dimethoxy-1,3,5-triazin-2-yl)-4-methyl-morpholinium chloride) (DMT-MM) for 30 min in MES buffer (pH 5.5), and reacted with 1.5 equivalents of 3,3′-dithiobis(propionic dihydrazide) DTP for 3 days. The disulfide-containing MC-DTP was dialysed (MWCO 12–14 kDa, Spectrum Labs) against 0.1 M NaCl for 1 day and DI water for 2 days. The disulfide reduction was performed at room temperature, with a large excess of dithiothreitol (DTT), prior to dialysis against 0.1 M NaCl at pH 4 for 1 day, and HCl-acidified water at pH 4 for 2 days, to yield thiolated MC (≈ 110–150 nmoles of thiol per mg of MC). The

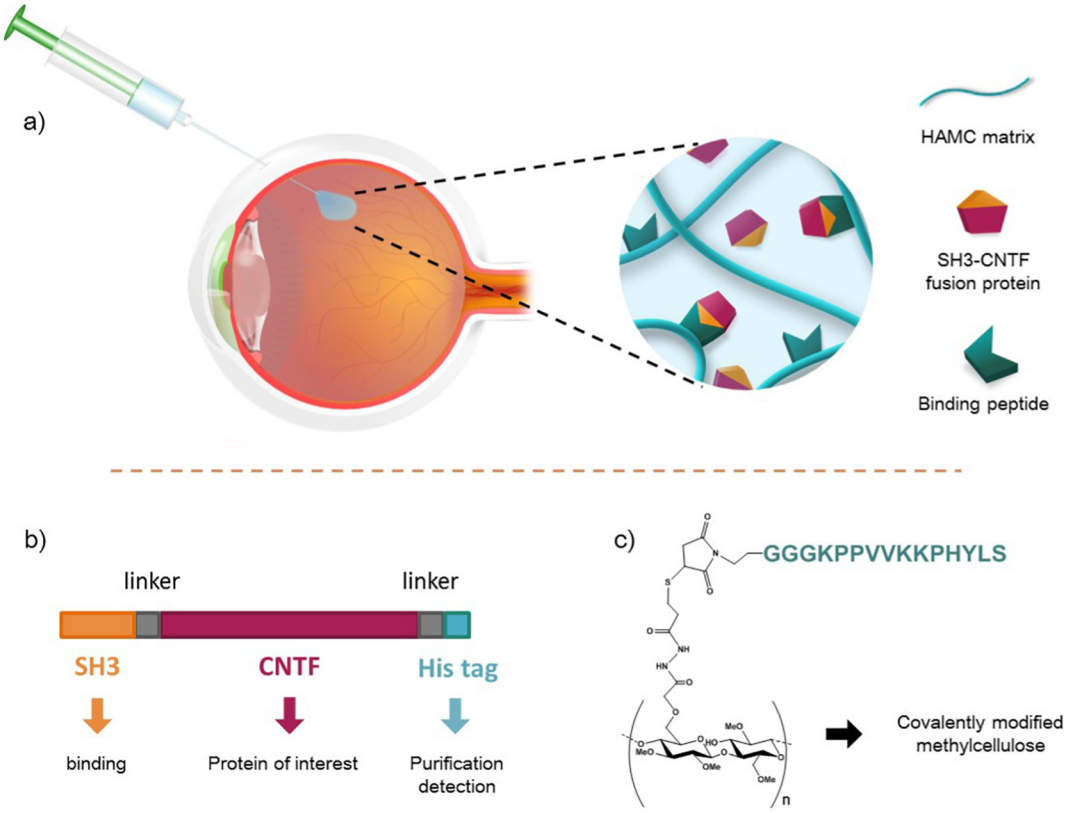

Fig. 1. a) Schematic of the intravitreal CNTF affinity-based release strategy. A physical thermogel composed of hyaluronan and methylcellulose, HAMC, is covalently modified with a peptide binding partner of the SH3 protein domain to allow the intravitreal sustained affinity release of a CNTF-SH3 fusion protein. b) The CNTF-SH3 fusion protein is recombinantly expressed from *E. coli*, with a His tag to facilitate purification. c) To immobilize the SH3 peptide binding partner of interest, the synthetic proline-rich peptide (sequence: GGGKPPVVKKPHYLS) is modified with a maleimide, prior to covalent grafting onto thiolated methylcellulose via Michael-type addition.

thiolated MC solution was adjusted to pH 6.8 and reacted overnight with 2 equivalents of maleimide-modified SH3-binding peptide via a Michael-type addition; the remaining free thiols were quenched with N-(2-hydroxyethyl) maleimide in excess (773,263 ALDRICH) for 24 h before dialysing the reaction solution (MWCO 100 kDa, Spectrum Labs) against 0.1 M phosphate buffer for 1 d and DI water for 2 d. The MC-peptide solution was then filter-sterilized, lyophilized and stored at −80 °C. The peptide content was evaluated by amino acid analysis.

2.4. Gel stability

A typical gel preparation for swelling/stability evaluation was, as follows: to prepare a HAMC 1/4 hydrogel, indicative of 1% and 4% (*w/v*) of hyaluronan (HA) and methylcellulose (MC), respectively, 4 mg of HA and 16 mg of MC were placed in a 2-mL Eppendorf tube. 400 µL of PBS were added, and the polymer mix was sequentially speed-mixed (SpeedMixer DAC 150 FV2; FlackTek Inc., Landrum, USA) for 2 min, microcentrifuged at max speed (14,000 rpm) for 10 s and kept on ice for 30 min, 2 times, prior to gentle shaking at 4 °C overnight. The pre-gel mix was centrifuged one more time for 2 min, and microcentrifuged for 2 min at max speed. Pre-gel formulations were transferred to a 500-µL Hamilton syringe equipped with a 22-gauge needle, and divided into 100-µL pre-gels in pre-weighed, 2-mL Eppendorf tubes. Using swinging buckets, the pre-gels were flattened by centrifugation (5 s; 3000 rpm) at 4 °C. The formulations were kept shaking gently for 15 min in a 37 °C incubator to allow complete thermogelation. The gel-containing tubes were weighed, and warm PBS (37 °C) was added to simulate release conditions and exposure to fluids. At specific time points (0, 2, 6, 24, 48 h; then 4, 7, 10 and 14 d), supernatants were removed, gel surfaces were carefully dried with wipes, and tubes were weighed. The swelling was determined as the ratio of a hydrogel mass at a given time point over its initial mass. Maximum swelling was determined as the highest mass ratio reached during the swelling study.

2.5. Thermogelation properties

Thermogelation data were collected using a TA Instruments AR1000 rheometer (New Castle, DE), equipped with a 1° acrylic cone (60 mm) and a Peltier plate for temperature control. A solvent trap was used to minimize evaporation during the measurements. Gels were first equilibrated for 5 min at 4 °C. Then, the loss tangent, tan(δ), defined as the ratio of shear loss modulus (G") and shear storage modulus (G'), was measured as a function of temperature, from 5 °C to 50 °C, with 5 °C increments stabilizing for 5 min each. The measurements were performed at 3 different angular frequencies in the terminal zone (0.01, 0.02 and 0.1 Hz), using 1% strain, which was confirmed to be in the linear viscoelastic region of the material studied.

2.6. Mathematical procedure for gel design

Using a previously reported mathematical model for affinity release systems, the theoretical diffusivity of the designed protein was first calculated. From the Stokes-Einstein equation and an approximation of the protein volume [40], the diffusivity of CNTF-SH3 at 37 °C, noted $D_{CNTF\text{-}SH3}$, was calculated to be $1.55\ 10^{-10}\ m^2\ s^{-1}$. Next, for a chosen release duration of 7 d (604,800 s), the required concentration of peptide, $C_{peptide}$, was determined using the following equation from our mathematical model [37]:

$$C_{peptide} = K_D * \left(\frac{t * D}{t^* * L^2} - 1 \right)$$

where t is the desired release duration (s); t* = 1, the dimensionless time for theoretical 100% release from the published master curve; $L = 4 \times 10^{-3}$ m, the thickness of the gel; D is the calculated diffusivity ($m^2 s^{-1}$), and $K_D = 2.7.10^{-5}$ M, the specific dissociation constant for the designed peptide and SH3.

To ensure 1% protein release detection, the total CNTF-SH3 concentration was adjusted based on the lower limit of detection by ELISA (0.025 μg.mL^{-1}). The total CNTF-SH3 concentration was set to 2.5 μg mL^{-1}, or 76.68 nM. Considering 900 μL of release medium, this corresponds to the encapsulation of 2.5 μg of CNTF-SH3 per 100 μL gel. This concentration was mathematically tested to confirm Regime 1 controlled release, using the following conditions, at the equilibrium:

$$\alpha = \frac{C_{free\ protein,0}}{C_{peptide}} \ (no\ condition\ on\ \alpha)$$

$$\beta = \frac{L^2 * k_{off}}{D} >> 1$$

$$\gamma = \frac{C_{free\ protein,0}}{K_D} << 1$$

where α, β and γ are three dimensionless parameters influencing the regime of release; $L = 4 \times 10^{-3}$ m is the thickness of the gel; $k_{off} = 10^4\ s^{-1}$ is an approximation of the dissociation rate constant; D is the diffusivity calculated above (in $m^2 s^{-1}$); $K_D = 2.7\ 10^{-5}$ M, the specific dissociation constant for the designed peptide and SH3; $C_{free\ protein,0}$ is the free-state protein concentration in an equilibrated gel.

The required free-state protein concentration, $C_{free\ protein,0}$, is calculated from the following K_D expression:

$$K_D = \frac{C_{protein,0} * C_{peptide,0}}{C_{complex}} = \frac{(C_{protein} - x_{eq}) * (C_{peptide} - x_{eq})}{x_{eq}}$$

where $C_{free\ protein,0}$ is the free-state protein concentration in an equilibrated gel; $C_{protein}$ = 76.68 nM, the desired total amount of protein in a gel; $C_{peptide}$ = 1.9 M, the calculated amount of immobilized peptide in a gel; $C_{complex}$ the amount of complexed protein with peptide (M); $K_D = 2.7\ 10^{-5}$ M, the specific dissociation constant for the immobilized peptide and SH3; and x_{eq}, the concentration of bound protein and peptide at the equilibrium.

2.7. HAMC Gel preparation

Each of HA, MC and MC-peptide was dissolved in deionized H_2O, sterile-filtered and lyophilized. To make 400 μL of peptide-modified HAMC 1/4, in a 2-mL Eppendorf tube, 4 mg of sodium hyaluronate (1.2–1.9 MDa; NovaMatrix), 9.82 mg of MC and 6.18 mg of peptide-modified MC were dissolved in 394.7 μL of PBS containing 2 mg mL^{-1} BSA and some EDTA-free Protease Inhibitor Cocktail (Sigma-Aldrich; a tablet per 10 mL). The polymer blend was speed-mixed (SpeedMixer DAC 150 FV2; FlackTek Inc., Landrum, USA) for 2 min, microcentrifuged at maximum speed (14,000 rpm) for 10 s and kept on ice for 30 min, repeated 3 times, prior to a final microcentrifugation for 2 min at maximum speed. 5.26 μL of CNTF-SH3 (10 μg) were added onto the polymer blend, which was subsequently speedmixed for 30 s, centrifuged for 2 min and left shaking at 4 °C overnight. The protein-containing pre-gel mix was centrifuged one more time for 2 min prior to use in the protein release study.

2.8. Release study and protein degradation

Gels were prepared as described above. An unmodified HAMC control was prepared, following the same formulation procedure without the incorporation of peptide-modified MC. Pre-gel formulations were transferred to a 500 μL Hamilton syringe equipped with a 22-gauge needle, and divided into 100 μL pre-gels in separate 2 mL Eppendorf tubes. Using swinging buckets, the pre-gels were flattened by centrifugation (5 s; 3000 rpm) at 4 °C. The formulations were kept in a 37 °C incubator with gentle shaking for 15 min to allow complete thermogelation. 900 μL of warm release medium was added to each tube, and the gels were kept in a 37 °C incubator with gentle shaking for the time of the release study. The supernatants were collected (and stored at −80 °C) at designated time points (0, 2, 6, 12, 24, 48 h, and 4, 7, 10 d), and replaced with 900 μL of new warm release medium.

Soluble CNTF-SH3 was used to evaluate protein degradation: CNTF-SH3 was diluted in release medium (0.25 μg mL^{-1}), aliquoted (500 μL) in 1.5-mL Eppendorf tubes, and kept at 37 °C with the releasing gels for the time of the study. At each time point, an aliquot was stored at −80 °C for future analysis. Similarly, as blank for analyses, release medium was kept at 37 °C, sampled at each time point and stored at −80 °C.

2.9. ELISA for CNTF-SH3

Duplicated standard samples of fresh CNTF-SH3, from 0.016–1.0 μg mL^{-1}, were prepared by serial dilution in fresh release medium. Released samples, degradation controls and release medium blanks from the release study were all quickly thawed (37 °C, 2 min) and kept on ice until use. 200 μL of each standard dilution (duplicates), samples (triplicates) and controls (triplicates), were plated into a 96-well Ni-NTA plate (Qiagen, Toronto, ON), and incubated for 2 h at 37 °C on an orbital shaker. The wells were washed 4 times with 300 μL of wash buffer (1× PBS + 0.05% Tween 20), gently shaken for 1 min, before vigorous tapping and blot drying of the plate on paper towels. 200 μL of primary anti-CNTF antibody solution (rabbit; 1:10000 dilution in 1× PBS + 0.2% BSA) were added to each well, prior to incubation at room temperature on orbital shaker for 1 h. The wells were washed 4 times following the aforementioned procedure. 200 μL of HRP-conjugated secondary antibody solution (anti-rabbit; 1:5000 dilution in 1× PBS + 0.2% BSA) were added to each well, prior to incubation at room temperature on orbital shaker for 45 min. The wells were washed again 4 times, and 100 μL of 2,2′-azino-bis(3-ethylbenzothiazoline-6-sulphonic acid) (ABTS) solution was added to each well, and incubated at room temperature on shaker for 20 min. The absorbance was measured at 405 nm with a wavelength correction at 650 nm. Protein concentration was calculated based on the linear range of a standard curve from the same plate, corrected with the protein degradation curve.

2.10. CNTF-SH3 bioactivity assay

Using a TF1-α cell proliferation assay, the CNTF-SH3 protein bioactivity was evaluated and compared to commercial CNTF in vitro. TF1-α cells were grown in RPMI with 10% (v/v) FBS, containing 2 ng mL^{-1} of recombinant human GM-CSF (life technology; REF PHC2015). The cells were then pelleted and re-suspended at a density of 2×10^5 cells mL^{-1} in RPMI with 10% (v/v) FBS (no GM-CSF). 50 μL of the cell solution were plated in a 96-well plate (10^4 cells well^{-1}). The proteins tested, namely commercial CNTF and expressed CNTF-SH3, were diluted to the desired concentrations (1, 10 and 100 ng mL^{-1}) in RPMI with 10% (v/v) FBS; and 50 μL of the different protein solutions were added to separate wells (3 wells per condition). The cells were incubated for 24, 48 and 72 h at 37 °C (5% CO_2), prior to PrestoBlue® fluorescence measurements. The experiment was performed on three biological replicates, using TF1-α cells grown and passaged independently, at least 3 times.

A similar study was performed on CNTF-SH3 released samples. Released samples were stored at −80 °C until the end of the release experiment. The concentration of CNTF-SH3 at each time point was assessed by ELISA, and all samples were diluted to 10 ng mL^{-1} using

RPMI with 10% (*v*/v) FBS. The concentration-matched samples were then filter-sterilized and tested for bioactivity using the aforementioned proliferation assay.

2.11. Animals

All experiments were approved by the University Health Network Research Ethics Board and adhered to the guidelines of the Canadian Council on Animal Care. Animal husbandry was in accordance with the Association for Research in Vision and Ophthalmology (ARVO) Statement for the Use of Animals in Ophthalmic and Vision Research. Animals were maintained under standard laboratory conditions and all procedures were performed in conformity with the University Health Network Animal Care Committee (protocol 3499.13). 67 C57BL/6 J mice (Charles River) of both sexes were used, all between 6 and 8 weeks old at the time of treatment.

2.12. Intravitreal injections

Animals were anesthetized by a mixture of ketamine (Vetalar, Boehringer Ingelheim) and medetomidine (Cepetor, Modern Veterinary Therapeutics) in sterile 0.9% NaCl administered intraperitoneally. Eyes were dilated using 1% tropicamide (Mydriacyl, Alcon) drops. A scleral incision was made in the dorsal side, posterior to the limbus using a 30-gauge sharp needle. Next, a blunt 32-gauge needle (Hamilton) was inserted tangentially into the vitreal space avoiding the lens. Injection optimization was performed by injection of 1 μL of HAMC mixed with blue food dye into the left eye using a nano-injector (Harvard Apparatus). The optimal rate of injection was found to be 0.5 μL min^{-1} and needle was held in place post-transplant for 2 min to minimize reflux.

2.13. RNA purification and quantitative RT-PCR (qPCR)

Mice were euthanized at 24 h and 7 d post-injection by carbon dioxide inhalation. Subsequently, retinas were dissected in PBS and flash frozen using dry ice. Next, total RNA was extracted using the RNeasy Mini Kit (Qiagen) according to manufacturer's directions. First-strand cDNA was synthesized using the QuantiTect Reverse Transcription Kit (Qiagen) as per manufacturer's directions, with and without reverse transcriptase to assess genomic contamination during downstream RT-PCR. For all samples, target gene mRNA levels were determined by quantitative RT-PCR (qPCR) using iQ SYBR Green Supermix (Bio-Rad) and a MyiQ iCycler (Bio-Rad). Primer pairs were designed using PRIMER-blast (http://www.ncbi.nlm.nih.gov/) or were previously published (Table S1). Primers were optimized using a 5-point standard curve of 2-fold diluted composite cDNA from relevant tissue and deemed acceptable with an $R^2 > 0.95$, a percent efficiency between 90 and 110%, a sharp single point melt curve, positive controls with C_t values > 10 cycle difference compared to no RT control samples, and expected amplicon size by agarose gel electrophoresis. All samples were run in triplicate, normalized to GAPDH, and quantified relative to the PBS injected animals.

2.14. Immunoblotting

Mice were euthanized at 24 h and 7 d post-injection by carbon dioxide inhalation. Following, total protein extracts were prepared from frozen adult mouse retinas by manual homogenization in ice-cold RIPA lysis buffer (50 mM Tris–HCl pH 7.4, 150 mM NaCl, 1% NP40, 0.1% SDS, 0.5% sodium deoxycholate, 10 mM NaF, 5 mM sodium citrate, 1.5 mM $MgCl_2$, 10 μM $ZnCl_2$) supplemented with a protease inhibitor cocktail (Roche) and phosphatase inhibitor cocktail (Thermo-Fisher). Homogenates were sonicated for 10 s at 4 °C, followed by centrifugation at 15,000 *g* for 20 min at 4 °C to sediment insoluble material. Protein samples were quantified via Bradford assay, resolved by denaturing SDS-PAGE on 4–20% Tris-acetate polyacrylamide gels (Bio-Rad), and blotted onto PVDF membranes (Bio-Rad) by electrophoretic transfer in Tris-glycine buffer containing 10% methanol and 0.05% SDS. Membranes were blocked with 5% BSA in Tris-buffered saline (TBS) for 1–2 h at room temperature, followed by overnight incubation at 4 °C with a 1:1000 dilution of mouse anti-STAT3 antibody (Cell Signaling Technology, Danvers, MA, USA) or a 1:2000 dilution of rabbit anti-P-STAT3 antibody (Cell Signaling Technology, Danvers, MA, USA), and subsequent incubation for 1–2 h at room temperature in a 1:10,000 dilution of donkey anti-mouse IgG (Sigma-Aldrich Canada Co., Oakville, ON, Canada) or donkey anti-rabbit IgG (Sigma-Aldrich Canada Co., Oakville, ON, Canada). Membranes were subjected to three 10 min washes in TBS following primary and secondary antibody incubation. Immunoblots of retinal protein extracts pooled from three mice were used for the analysis of STAT3 and P-STAT3 protein levels.

2.15. Immunohistochemistry

Mice were euthanized at 7 d post-injection by carbon dioxide inhalation. Subsequently, mice were exsanguinated with PBS (0.14 M NaCl, 2.5 mM KCl, 0.2 M Na_2HPO_4, 0.2 M KH_2PO_4) and transcardially perfused with 4% paraformaldehyde (PFA). Eyes were then marked with a silver nitrate stick on the dorsal part of the cornea before enucleating. Eyes were fixed for an additional 30 min in 4% PFA on ice and then cryoprotected overnight in 30% sucrose at 4 °C in PBS. Next, tissues were equilibrated in 50:50 *v*/v 30% sucrose in PBS: OCT (Tissue-Tek) for 1 h and subsequently oriented and embedded in plastic molds. Tissue blocks were stored in −80 °C. Tissue was sectioned at 20 μm thickness onto Superfrost Plus slides (Fisher Scientific) on a Leica cryostat and air-dried for 1 h before being stored in a slide box with desiccant at −20 °C. For immunocytochemistry, sections were blocked with 10% donkey serum (DS) (Sigma Aldrich, Oakville, Canada, www.sigmaaldrich.com) 0.3% Triton-X in PBS for 1 h at room temperature. Primary antibodies against GFAP (1:500, Abcam) and Cone arrestin (1:1000, Millipore) were diluted in 5% DS 0.15% Triton-X in PBS for overnight staining of retina sections at 4 °C. After 3 washes with PBS, sections were incubated with fluorescent secondary antibody diluted in 5% DS 0.15% Triton-X in PBS for 1 h at room temperature in a light protected humidified box. Nuclei were counterstained with fluorescent DNA-binding dye, Hoechst 33342 (Life Technologies). Slides were washed and glass coverslips were mounted with DAKO mounting media.

2.16. Statistical analysis

All in vitro data are presented as mean ± standard deviation. All in vivo data are presented as mean ± standard error of the mean (S.E.M.). Statistical analyses were performed using Excel and statistical significance was determined using a Student's *t*-test when applicable.

3. Results

3.1. HAMC 1/4 is the optimal hydrogel formulation based on minimal-swelling and stability

To investigate the use of a peptide-modified HAMC as an intravitreal hydrogel for CNTF affinity release, we first studied the effect of HAMC composition on hydrogel swelling and stability. Using filter-sterilized materials, a systematic swelling study of all combinations of HA and MC at 0, 1, 3 and 6% (*w*/*v*) was performed at 37 °C (Fig. 2a). When comparing the maximum swelling as a function of either HA or MC concentration, HA has the dominant effect, with swelling increasing with HA concentration in a linear fashion (Fig. S1). Interestingly, the swelling behavior of HAMC is independent of the ratio of the two polymers. To minimize swelling, 1% (w/v) HA was selected for further studies of stability, thermogelation and affinity release.

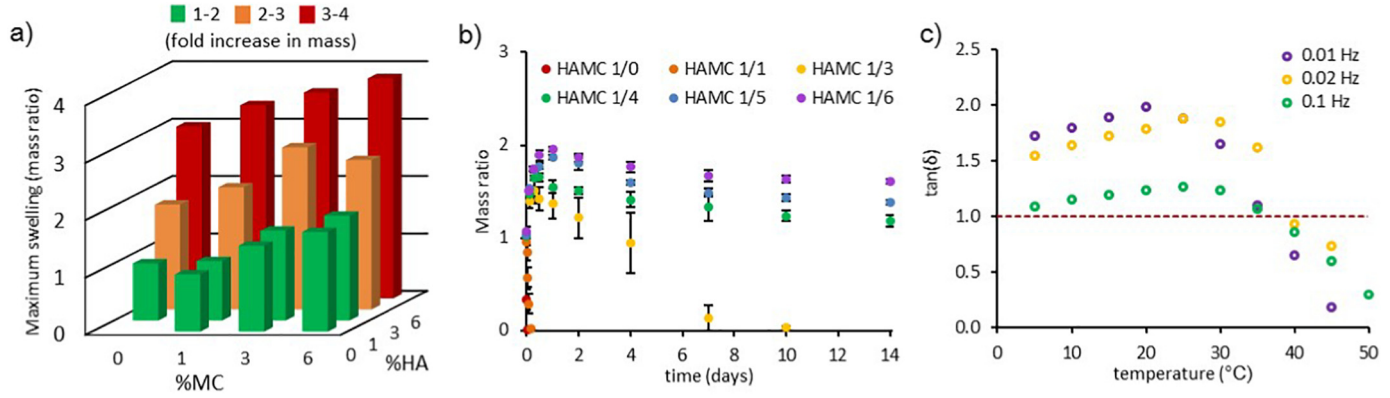

Fig. 2. Optimization and characterization of the HAMC thermogel for the affinity-release strategy. a) Maximum swelling characterization of various formulations of hyaluronan and methylcellulose (HAMC) at 37 °C, distinguishing between increases in mass: 1–2 fold increase (green), 2–3 fold increase (orange) and 3–4 fold increase (red). b) Stability study of various HAMC formulations at 37 °C, with HA concentration fixed to 1% (*w/v*). c) Thermogelation evaluation of the optimal HAMC 1/4, measuring the loss tangent, tan(δ), defined as the ratio of shear loss modulus (G") and shear storage modulus (G'). (For interpretation of the references to colour in this figure legend, the reader is referred to the web version of this article.)

We investigated the effect of the MC concentration on thermogel stability at 37 °C, given that MC chains form hydrophobic physical crosslinks. We found that 4% (*w/v*) MC is the minimal concentration necessary to achieve at least two weeks of stability (Fig. 2b). While higher MC concentrations also result in stable gels, higher polymer content increases viscosity, which makes injection difficult. Thus, HAMC 1/4 was selected as the best candidate for both stability and minimal swelling. To confirm the inverse thermogelation mechanism associated with MC, the dynamic shear storage and loss moduli of HAMC 1/4, as a function of temperature, were further evaluated. The entanglement of HMW HA chains can produce transient pseudo-viscoelastic properties, which depend on the polymer concentration and the angular frequency during the measurements [41,42]. Using 1% (*w/v*) HA, we confirmed that evaluating HAMC gelation at a frequency ≥ 1 Hz distorts the results (Fig. S2). To better assess the gelation temperature, the loss tangent, tan(δ), defined as the ratio of shear loss modulus (G") to shear storage modulus (G'), was measured at 3 different angular frequencies in the terminal zone of HMW HA (0.01, 0.02 and 0.1 Hz) (Fig. 2c). While our measurements do not show a single intersection, which is the theoretical indication of an exact gelation point, all curves show similar trends, with a clear decrease in loss tangent above 25 °C, and consistently reaching gel state (tan(δ) ≤ 1) in the range of 35–40 °C. Furthermore, when the thermogel was stabilized at 37 °C and subsequently incubated at 4 °C, we observed rapid gelation reversal and complete dissolution within hours (Fig. S3).

3.2. Expressed CNTF-SH3 is bioactive and stable

CNTF-SH3 was successfully expressed as a fusion protein of CNTF with SH3, as shown by SDS-PAGE (Fig. 3a), with a single band between 25 and 37 kDa. Further characterization by mass spectrometry revealed a mass of 32,459 g mol^{-1} (Fig. 3b), close to the expected 32,600 g mol^{-1}, suggesting minor discrepancies in amino acids and/or impurities.

The bioactivity of the CNTF-SH3 was assessed in vitro using the TF1-α erythroleukemic cell proliferation assay over a range of protein concentrations (1 to 100 ng mL^{-1}). At all the concentrations tested, the fusion protein significantly increased cell proliferation compared to no treatment (Fig. 3c). Furthermore, the CNTF-SH3 bioactivity was not significantly different from that of a commercial CNTF at the same concentration.

To gain insight into the stability of CNTF and CNTF-SH3, the proteins were subjected to thermal stability experiments, using static light scattering (SLS) to characterize melting temperatures (T_m) and protein unfolding. While the reference CNTF shows a single melting temperature at 53 °C, CNTF-SH3 possesses two successive inflection points at 53 °C and 75 °C, reflecting the successive unfolding of each of its domains – first CNTF and then SH3 (Fig. 3d). To further evaluate the stability of CNTF-SH3 in release conditions, aliquots of fusion protein solution were subjected to similar processing steps to release samples (i.e., dilution, incubation and storage), and tested for stability by ELISA (Fig. 3e). The normalized results show that after an initial ≈ 30% decrease, protein detectability remains consistent over the 10 d experiment.

3.3. A mathematical model allows the design of controlled release

To sustain the release of CNTF-SH3 from HAMC, a maleimide-modified SH3-binding peptide, GGGKPVVKKPHYLS, with a K_D of 2.7 × 10^{-5} M, was immobilized onto MC (110 nmol mg^{-1}), as previously reported [36,39]. To achieve the desired release profile of CNTF release in 7 days, we used a published mathematical model [37]. We first determined the dimensionless time, t*, from the reported master curve model (t* = 1). The concentration of immobilized peptide required in the hydrogel to achieve the desired release profile was then calculated according to the following equation:

$$C_{peptide} = K_D\left(\frac{t*D}{t^{*}*L^2} - 1\right)$$

where L = 4 × 10^{-3} m is the thickness of the gel; D = 1.55 10^{-10} m^2 s^{-1} is the calculated protein diffusivity; and K_D = 2.7 10^{-5} M is the specific dissociation constant for the designed peptide and SH3.

The designed release system of HAMC-peptide and CNTF-SH3 resulted in the predicted protein release profile, and the release was slower at all time points compared to that of unmodified HAMC and CNTF-SH3 (Fig. 4a). To compare the release rates, the cumulative protein release was plotted against the square root of time, where the slope of the linear portion is proportional to the apparent protein diffusivity (Fig. 4b). The calculated diffusion coefficients, k_1 and k_2, show a 2.44-fold decrease ($p \leq .01$) in apparent protein diffusivity in the modified HAMC-peptide compared to the unmodified HAMC, confirming controlled release. The Fickian diffusion phase was extended in HAMC-peptide to 48 h vs. 24 h for HAMC. However, after 7 days, the cumulative released fraction reached a plateau at 49.2 ± 1.5% from HAMC-peptide vs. 80.6 ± 9.6% from unmodified HAMC. The hydrogels were subsequently dissolved at 4 °C to quantify the remaining free protein in the gels (Fig. 4c). In the unmodified gel, 7.9 ± 0.8% of free CNTF-SH3 was detected, enabling us to account for 88.5 ± 9.0% of the initial amount of encapsulated protein. In the modified HAMC-peptide, however, the unbound fraction of the remaining CNTF-SH3 appeared to

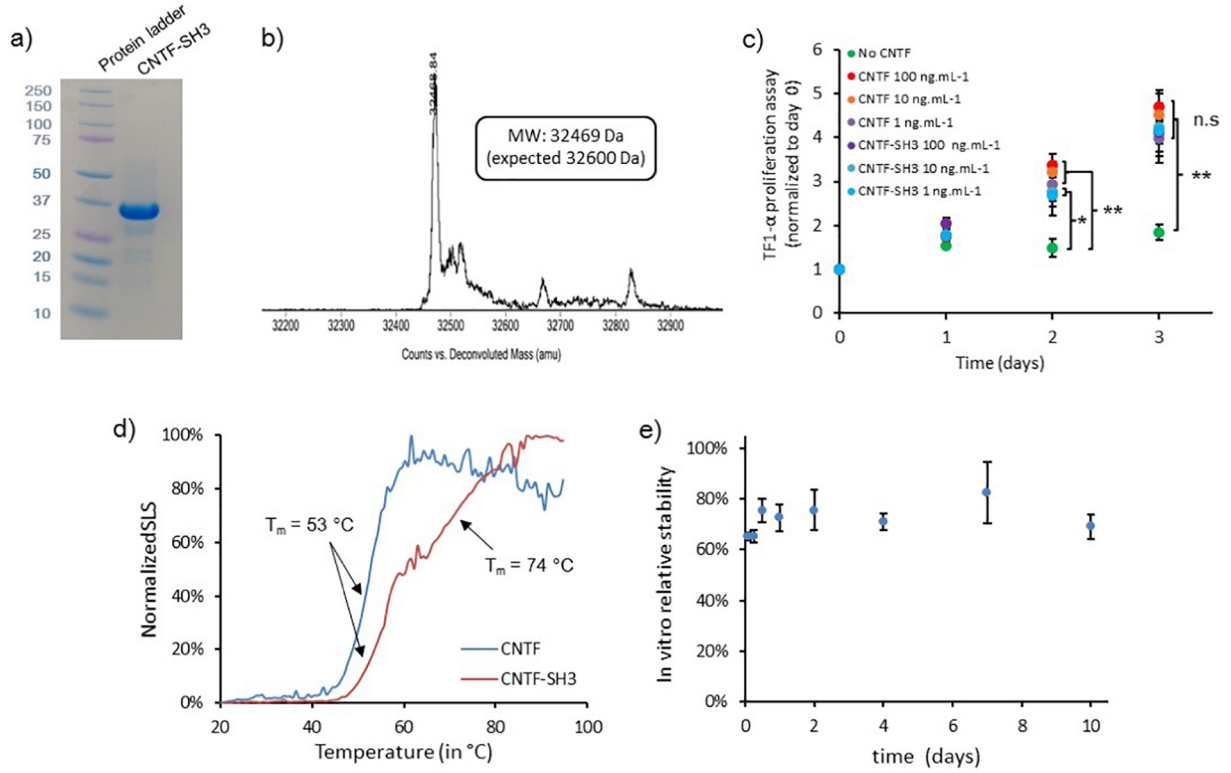

Fig. 3. Characterization of the CNTF-SH3 fusion protein expression and stability. a) SDS-PAGE of recombinantly expressed CNTF-SH3 from E.coli, after successive purifications by nickel affinity column and flash protein liquid chromatography. b) Mass spectrum of the purified CNTF-SH3. c) In vitro evaluation of the bioactivity of CNTF-SH3, using TF1-α erythroleukemic cell proliferation assay. Various concentrations of the recombinant CNTF-SH3 protein (1, 10 and 100 ng mL^{-1}) were tested for cell proliferation, and compared to similar concentrations of commercially available CNTF. Using PrestoBlue, cell metabolic activity was measured as a proxy for cell proliferation. The metabolic activity is expressed as fold change relative to time zero, shown as mean ± standard deviation (n = 3 biological replicates; one-way ANOVA, *p < .05, **p < .01 ***p < .001). d) Thermal stability of CNTF vs CNTF-SH3, measured by static light scattering (SLS), showing melting temperatures (T_m) as indications of protein domain unfolding. e) Stability of released CNTF-SH3 over time measured by CNTF ELISA.

be below the lower limit of detection, suggesting a strong shift of the equilibrium towards the bound state of the molecule that restricts further release.

The bioactivity of released CNTF-SH3 was confirmed using the TF1-α erythroleukemic cell proliferation assay (Fig. 4d). The normalized proliferation induction capacity of the release samples showed an initial bioactivity of approximately 80% relative to that of the fresh protein. The bioactivity then decreased to 73.1 ± 1.8% at day 4 and to 61.3 ± 3.1% at day 7.

3.4. Intravitreal, affinity-released CNTF is successfully delivered to the retina

To test the feasibility of intravitreal protein delivery from our bioengineered hydrogel, intravitreal injections were performed in wild-type mice. In a preliminary experiment, HAMC was mixed with blue dye to visualize the gel, showing successful injection in a mouse vitreous (Fig. 5a). Each of the following formulations was injected into the vitreous (1 µL): HAMC-peptide/CNTF-SH3, CNTF-SH3 alone, HAMC-peptide vehicle alone, commercial hCNTF alone or PBS. All CNTF groups were tested at a protein concentration of 250 µg mL^{-1}, which is a typical CNTF concentration delivered to the eye [43,44]. qPCR was performed on retinal tissues from days 1 and 7 post-treatment, where the transient upregulation of Stat-1 and Stat-3 genes and downregulation of phototransduction transcripts (e.g., rhodopsin, S-opsin, M-opsin, Gnat 1 and 2) were evaluated (Fig. 5b). One day following treatment, HAMC-peptide/CNTF-SH3, CNTF-SH3 and hCNTF groups all showed a significant increase in Stat1 and Stat3 expression compared to the PBS control, along with the expected downregulation of all phototransduction transcripts. After 7 days, all Stat1, Stat3 and phototransduction transcript levels essentially returned to baseline levels, with statistically significant changes observed for rhodopsin, S-opsin, M-opsin Gnat-1 and Gnat-2 for CNTF samples; however, since the differences are small, their biological significant remains unclear.

The effect of CNTF-SH3 was further corroborated by western blot (Fig. 5c). After one day, expression levels of phospho-Stat3 increased in HAMC-peptide/CNTF-SH3, CNTF-SH3 and hCNTF, confirming the bioactivity of released CNTF-SH3 in vivo. At day 7, the expression of phospho-Stat3 decreased in all groups, with only minimal expression observed in HAMC-peptide/CNTF-SH3 and hCNTF treated mice.

At 7 days after injection, retinas from each group were analyzed by immunohistochemistry for Cone arrestin and GFAP for the cone photoreceptors and Müller glia, respectively (Fig. 5d). The retinal structure was preserved and the outer nuclear layer (ONL) thickness maintained after treatment.

4. Discussion

Intravitreal affinity-based release constitutes an interesting, yet unexplored, alternative to conventional bolus intravitreal injection for protein delivery to the retina. Bolus delivery can cause an increase in intravitreal pressure and infusion pumps are prone to infection [45], necessitating a slow release formulation. While most local delivery systems for similar applications have simply reproduced natural interactions by incorporating ECM components (e.g., heparin) or their binding domains, we designed a more specific and tunable affinity by bioengineering both protein and scaffold to tailor release profile.

We showed that the thermogel swelling properties are consistent with the structures of the two mixed polysaccharides, reflecting the hydrophobicity of MC, which enables physical crosslinks, and the

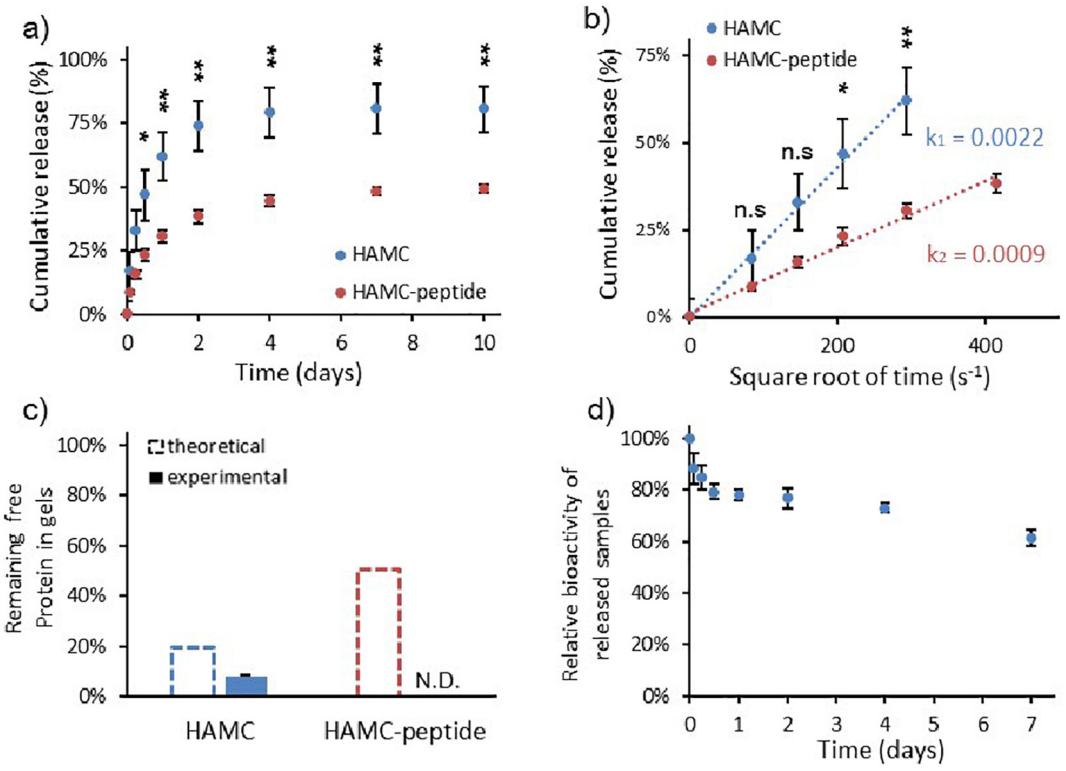

Fig. 4. Evaluation of the controlled release and bioactivity of CNTF-SH3. a) Cumulative release of CNTF-SH3 from unmodified HAMC vs SH3-binding peptide-modified HAMC ($n = 3$, mean ± standard deviation). b) Fickian diffusion phases from release profiles in (a). The slopes, K_1 and K_2, are proportional to apparent protein diffusivity through the gel. (n = 3, mean ± standard deviation). c) Quantification of free protein remaining in unmodified HAMC vs peptide-modified HAMC, comparing theoretical amounts calculated from release profile (dashed borders) to experimental amounts measured by ELISA (solid fill). N.D. = not detected. d) In vitro evaluation of the bioactivity of released CNTF-SH3, using a TF1-α erythroleukemic cells proliferation assay. Released samples were concentration-matched to 10 ng mL^{-1}. Using PrestoBlue, the cell metabolic activity was measured as a proxy for cell proliferation. The metabolic activity is expressed as fold change relative to fresh protein (n = 3; mean ± standard deviation). Statistical significance was determined using a Student's *t*-test when applicable. n.s – not significant, * $p < .05$, ** $p < .01$, *** $p < .001$.

hydrophilicity of HA, which results from the negative charges of its carboxylate groups at physiological pH. Notwithstanding the swelling behaviour of HA, it is crucial in the design of our intravitreal hydrogel as it possesses unique anti-inflammatory properties [46], is a major component of the vitreous humor [47,48], and its high molecular weight increases the viscosity of the injectable material, thereby enhancing gelation while preventing backflow upon injection. Interestingly, our rheometry experiments reveal that the tan(δ) of HAMC 1/4 increases from 4 to 25 °C, reflecting the typical thermogelation property of HMW HA [49] and suggesting that the lowest viscosity for ease of injection is close to room temperature. Together our results demonstrate that HAMC 1/4 is a minimally-swelling, yet stable, hydrogel, with an inverse thermogelation temperature matching body temperature.

Using a series of concentrations relevant for in vivo delivery [7,44], CNTF-SH3 demonstrated similar bioactivity to commercial CNTF. Our experiments also show, for the first time, the successive unfolding of each domain of an SH3-containing fusion protein, confirming that the structures of both domains are maintained upon recombinant expression. A melting temperature of 75 °C is in good agreement with the reported high denaturation temperature of various SH3 domains at physiological pH, in the range of 60–80 °C [50,51], further supporting these findings. More importantly, both CNTF and CNTF-SH3 are thermally stable at body temperature (37 °C), which makes them suitable for prolonged release in vivo. Together with the CNTF-SH3 stability study in release conditions, the bioactivity of CNTF-SH3 released samples revealed initial, partial protein degradation, likely due to unfolding and/or aggregation from the processing (mixing and repeated freeze/thawing). Most importantly, this highlights that ≥70% of the protein molecules remain intact, are available for release, and maintain their bioactivity over at least one week.

The SH3 affinity-based release strategy has been applied for the delivery of various factors [36,38,52], with repeated optimization of both peptide and protein concentrations. The present study used a published mathematical model [37] to achieve the desired release profile of CNTF-SH3 in 7 days; however, a release plateau was observed after 7 d, reflecting a limitation of this affinity-based release system. These results are consistent with previous release studies, where, for example, the release of fibroblast growth factor 2-SH3 (FGF2-SH3) was limited to 44.2% [36], and that of chondroitinase ABC-SH3 (ChABC-SH3) plateaued at approximately 50% [38]. Given our inability to detect free protein in the dissolved HAMC-peptide gels after the 7-day release study, it is likely that there was a shift in equilibrium to the bound state during the CNTF-SH3 release study. The present system used a lower protein concentration (0.77 μM vs 4.56 μM) and a higher peptide concentration (1907 μM vs 456 μM) than previous studies; yet, a similar release profile was observed. The similar release profile confirms the model prediction that the time scale of release is independent of the protein concentration in the controlled release regime. With a tested protein-to-peptide ratio of 2477:1 vs 100:1 in previous studies, these results also demonstrate that the release is independent of protein-to-peptide ratios. Using a theoretical peptide density to successfully sustain the release of CNTF-SH3 from a thermogel demonstrates the power of mathematically designing materials for controlled release, allowing us to bypass trial and error optimization. The effective release of an arbitrary concentration of protein also confirmed that, under the appropriate regime of protein release, this affinity release is independent of protein concentration.

To test the feasibility of intravitreal protein delivery from our

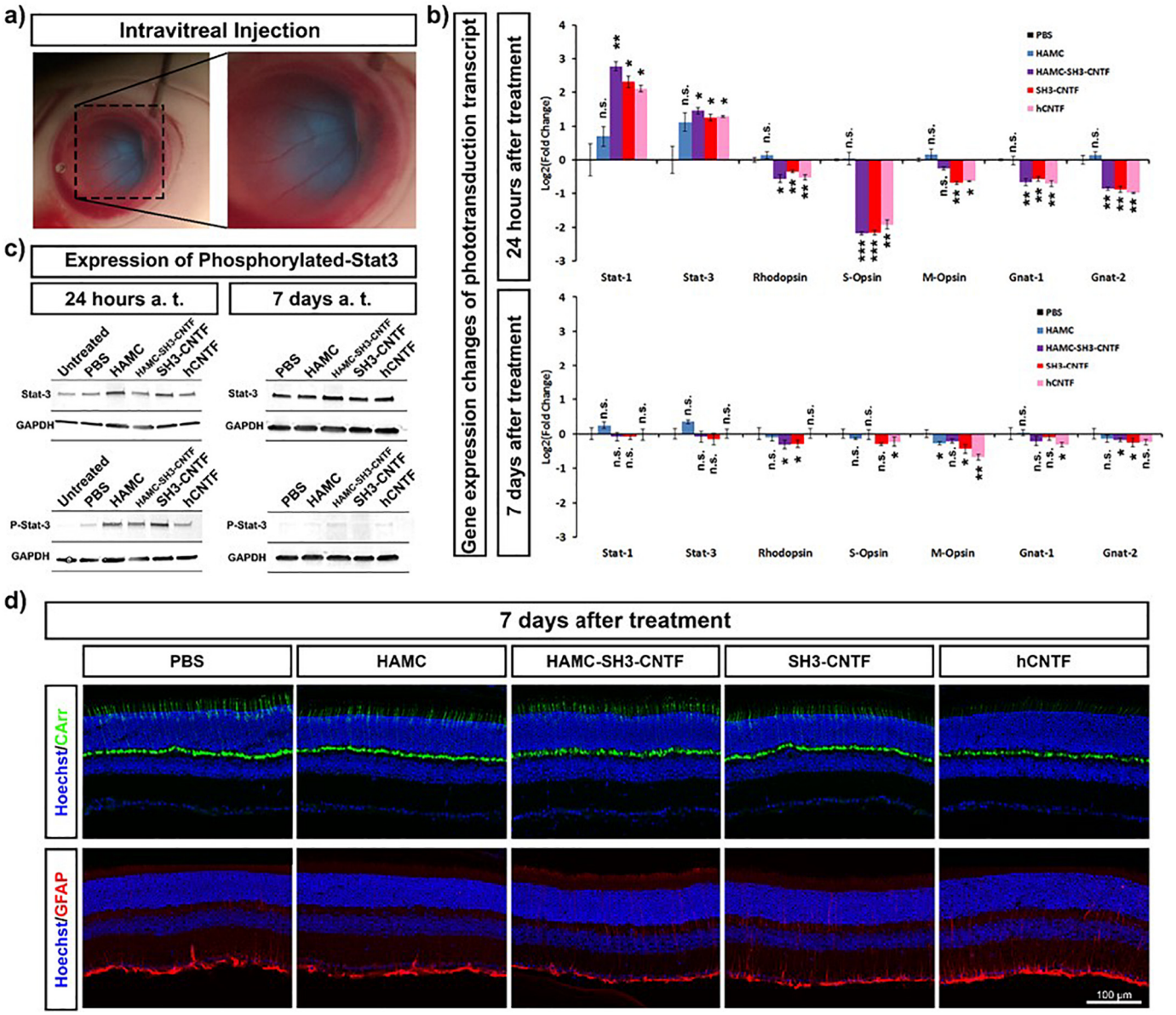

Fig. 5. In vivo evaluation of CNTF-SH3 intravitreal release from HAMC, compared to PBS, HAMC, CNTF-SH3 alone and commercial human CNTF. a) Fundus photograph of intravitreal injection of 1 µL of a blue-stained HAMC during the delivery in an albino mouse eye. b) Evaluation by qPCR of the transient effects of CNTF-SH3 delivery on the expression of Stat1, Stat3, and various phototransduction genes (rhodopsin, S-opsin, M-opsin, Gnat 1 and Gnat 2) relative to PBS injected eyes. c) Immunoblotting evaluation of the transient upregulation of Stat3 phosphorylation upon CNTF-SH3 delivery, using GAPDH as the housekeeping protein. d) Immunohistochemical analysis of retinal tissues from each group tested, 7 days post-treatment, staining for Hoechst (nuclei, blue), Cone arrestin (Carr for cone photoreceptors, green) and glial fibrillary acidic protein (GFAP for astrocytes/glia, red). n.s. – not significant, $*p < .05$, $**p < .01$, $***p < .001$. (For interpretation of the references to colour in this figure legend, the reader is referred to the web version of this article.)

bioengineered hydrogel, intravitreal injections were performed in mice. We chose to study local, sustained release of CNTF because of the numerous studies showing tissue and functional benefit in pre-clinical models where CNTF transiently downregulates the visual cycle and thereby slows down retinal degeneration [7,43,53,54]. Too much CNTF may lead to temporary vision loss, which argues against bolus injection and for sustained release within a therapeutic window [44]. Tests on a disease model with recovery evaluation would be ideal; however, anesthesia, intravitreal injection and light exposure during surgical microscopy provoke corneal opacification and different grades of cataracts [55–59], rendering visual function tests, such as electroretinography, extremely difficult. Therefore, we used wildtype mice as they are commonly used to unambiguously measure CNTF biological [44,53,54,60].

The newly designed CNTF-SH3 is bioactive in vivo, showing expected upregulation of Stat1 and Stat3 expression and downregulation of all phototransduction transcripts. Importantly, the in vivo bioactivity of released CNTF-SH3 is similar to that of commercial hCNTF, corroborating the in vitro results, and demonstrating, for the first time, both the successful intravitreal release of a protein from an affinity-based hydrogel, and its delivery from the vitreous to the retina. Further investigation by western blot showed increased expression levels of phospho-Stat3 in HAMC-peptide/CNTF-SH3, CNTF-SH3 and hCNTF, in agreement with the reported mechanism of action of CNTF [54,61].

After 7 days, Stat1/3 and phototransduction transcript levels returned to baseline, along with the decrease in phospho-Stat3 expression, which is indicative of the reversibility of the CNTF mechanism on the retina, as previously shown [44,54]. The lack of a prolonged effect from the affinity released CNTF-SH3 may be due to limited protein

availability at 7 days. While the in vitro data show bioactive CNTF at day 7, only 50% of the total loaded protein can be accounted for, suggesting that insufficient protein was released to the retina to achieve biological effect at 7 days. Possible discrepancies in release profile and degradation rate between in vitro and in vivo experiments could also explain our findings.

Surprisingly, the delivery of HAMC-peptide alone noticeably increased Stat1 and Stat3 expression levels, and upregulated Stat3 phosphorylation. This, however, did not affect the phototransduction transcript levels. By increasing the phospho-Stat3 expression without downregulating the visual cycle gene expression, the HAMC-peptide control data highlight the necessity of activating of other pathways, such as MAPK/ERK and PI3K-AKT, to promote neuronal survival [61–64]. The unexpected bioactivity of the delivery vehicle alone suggests that the scaffold and therapeutic can act synergistically to induce positive cell responses and regeneration. Unmodified HAMC 0.5/0.5 was previously tested for subretinal injection [65], where it too showed a biological benefit of pro-survival to transplanted cells through a CD44-mediated mechanism.

CNTF has repeatedly been reported to induce transient photoreceptor outer segment shortening [7,44,54]. While we did not observe this phenomenon, the ONL thickness was preserved 7 days after CNTF-SH3 treatment and photoreceptor gene expression was reversible after CNTF-SH3 delivery, indicating long-term effective restoration of photoreceptor morphology. Moreover, the multi-step chemistry developed for peptide immobilization to HAMC was safe and compatible with intravitreal injections. While beyond the scope of this study, the intravitreal protein release system will be tested in the future in disease models (e.g., rd1, rd10 rodent models) [66,67].

Importantly, our hydrogel-based delivery system is a platform technology that has been tested in vitro with IGF-1, FGF2 and in other models of disease for chABC [36,38,52,68]. Herein, we demonstrate not only in vitro, but in vivo release of CNTF, emphasizing the versatile nature of the SH3-fusion protein / SH3 binding peptide-modified hydrogel system for local, sustained release. We can extend this platform technology to other proteins of interest [69–72], specifically where sustained release for 1–2 weeks is beneficial.

5. Conclusions

We report the first demonstration of intravitreal protein release from a hydrogel and the first example of intravitreal affinity-based release with bioactive CNTF-SH3 to the retina. Using a mathematical model to predict release, we show sustained release of bioactive CNTF-SH3 for 7 d in vitro. We demonstrate the safety of the delivery system for intravitreal delivery, opening an entirely new route for hydrogel-based, intravitreal protein delivery.

Acknowledgments

We are grateful to members of the Shoichet lab for thoughtful review of this manuscript, and thank Dr. Malgosia Pakulska for her help with CNTF-SH3 expression. We are grateful to the following for funding this research: The Canada First Research Excellence Fund to the University of Toronto's Medicine by Design (to MSS and VW) and the Ontario Institute for Regenerative Medicine (to VW and MSS). Molly Shoichet also acknowledges support as a Tier 1 Canada Research Chair in Tissue Engineering.

Appendix A. Supplementary data

Supplementary data to this article can be found online at https://doi.org/10.1016/j.jconrel.2018.11.012.

References

[1] S. Azadi, et al., CNTF + BDNF treatment and neuroprotective pathways in the rd1 mouse retina, Brain Res. 1129 (1) (2007) 116–129.
[2] A. Kimura, et al., Neuroprotection, Growth Factors and BDNF-TrkB Signalling in Retinal Degeneration, Int. J. Mol. Sci. 17 (9) (2016) 1584.
[3] M.M. Lavail, et al., Multiple growth factors, cytokines, and neurotrophins rescue photoreceptors from the damaging effects of constant light, Proc. Natl. Acad. Sci. 89 (23) (1992) 11249–11253.
[4] J.M. Ogilvie, J.D. Speck, J.M. Lett, Growth Factors in Combination, but not Individually, rescue rd Mouse Photoreceptors in Organ Culture, Exp. Neurol. 161 (2) (2000) 676–685.
[5] A. Urtti, Challenges and obstacles of ocular pharmacokinetics and drug delivery, Adv. Drug Deliv. Rev. 58 (11) (2006) 1131–1135.
[6] D. Boyer, et al., Anti-Vascular Endothelial Growth Factor Therapy for Diabetic Macular Edema, vol. 4, (2013), pp. 151–169.
[7] R. Wen, et al., CNTF and retina, Prog. Retin. Eye Res. 31 (2) (2012) 136–151.
[8] D.G. Birch, et al., Randomized Trial of Ciliary Neurotrophic factor Delivered by Encapsulated Cell Intraocular Implants for Retinitis Pigmentosa, Am J. Ophthalmol. 156 (2) (2013) 283–292.e1.
[9] P.A. Sieving, et al., Ciliary neurotrophic factor (CNTF) for human retinal degeneration: phase I trial of CNTF delivered by encapsulated cell intraocular implants, Proc. Natl. Acad. Sci. U. S. A. 103 (10) (2006) 3896–3901.
[10] W. Tao, et al., Encapsulated cell-based delivery of CNTF reduces photoreceptor degeneration in animal models of retinitis pigmentosa, Invest. Ophthalmol. Vis. Sci. 43 (10) (2002) 3292–3298.
[11] www.aao.org/eyenet/academy-live/detail/phase-2-cntf-trial-shows-promise-in-people-with-ma.
[12] E.Y. Chew, et al., Ciliary neurotrophic factor (CNTF) for macular telangiectasia type 2 (MacTel): results from a phase I safety trial, Am J. Ophthalmol. 159 (4) (2015) 659–666 (e1).
[13] D.G. Birch, et al., Long-term follow-up of patients with Retinitis Pigmentosa Receiving Intraocular Ciliary Neurotrophic factor Implants, Am J. Ophthalmol. 170 (2016) 10–14.
[14] V. Delplace, J. Obermeyer, M.S. Shoichet, Local Affinity Release, ACS Nano 10 (7) (2016) 6433–6436.
[15] D., W.M, et al., Fibrin matrices with affinity-based delivery systems and neurotrophic factors promote functional nerve regeneration, Biotechnol. Bioeng. 106 (6) (2010) 970–979.
[16] A.K. Jha, et al., Molecular weight and concentration of heparin in hyaluronic acid-based matrices modulates growth factor retention kinetics and stem cell fate, J. Control. Release 209 (2015) 308–316.
[17] D.B. Pike, et al., Heparin-regulated release of growth factors in vitro and angiogenic response in vivo to implanted hyaluronan hydrogels containing VEGF and bFGF, Biomaterials 27 (30) (2006) 5242–5251.
[18] C.C. Rider, Heparin/heparan sulphate binding in the TGF-beta cytokine superfamily, Biochem. Soc. Trans. 34 (2006) 458–460 Pt 3.
[19] S.E. Sakiyama-Elbert, J.A. Hubbell, Development of fibrin derivatives for controlled release of heparin-binding growth factors, J. Control. Release 65 (3) (2000) 389–402.
[20] N.X. Wang, et al., Using Glycosaminoglycan/Chemokine Interactions for the Long-Term delivery of 5P12-RANTES in HIV Prevention, Mol. Pharm. 10 (10) (2013) 3564–3573.
[21] I. Freeman, S. Cohen, The influence of the sequential delivery of angiogenic factors from affinity-binding alginate scaffolds on vascularization, Biomaterials 30 (11) (2009) 2122–2131.
[22] M.R. Battig, B. Soontornworajit, Y. Wang, Programmable Release of Multiple Protein Drugs from Aptamer-Functionalized Hydrogels via Nucleic Acid Hybridization, J. Am. Chem. Soc. 134 (30) (2012) 12410–12413.
[23] M.M. Pakulska, et al., Encapsulation-free controlled release: Electrostatic adsorption eliminates the need for protein encapsulation in PLGA nanoparticles, Sci. Adv. 2 (5) (2016).
[24] A. Bochot, E. Fattal, Liposomes for intravitreal drug delivery: a state of the art, J. Control. Release 161 (2) (2012) 628–634.
[25] J.J. Kang-Mieler, C.R. Osswald, W.F. Mieler, Advances in ocular drug delivery: emphasis on the posterior segment, Expert Opin. Drug Deliv. 11 (10) (2014) 1647–1660.
[26] U.B. Kompella, et al., Nanomedicines for back of the eye drug delivery, gene delivery, and imaging, Prog. Retin. Eye Res. 36 (2013) 172–198.
[27] J. Jin, et al., Anti-inflammatory and antiangiogenic effects of nanoparticle-mediated delivery of a natural angiogenic inhibitor, Invest. Ophthalmol. Vis. Sci. 52 (9) (2011) 6230–6237.
[28] K. Park, et al., Nanoparticle-mediated expression of an angiogenic inhibitor ameliorates ischemia-induced retinal neovascularization and diabetes-induced retinal vascular leakage, Diabetes 58 (8) (2009) 1902–1913.
[29] T. Sakai, et al., Prolonged protective effect of basic fibroblast growth factor-impregnated nanoparticles in royal college of surgeons rats, Invest. Ophthalmol. Vis. Sci. 48 (7) (2007) 3381–3387.
[30] C.-H. Wang, et al., Extended release of bevacizumab by thermosensitive biodegradable and biocompatible hydrogel, Biomacromolecules 13 (1) (2012) 40–48.
[31] X. Xu, et al., Sustained release of avastin® from polysaccharides cross-linked hydrogels for ocular drug delivery, Int. J. Biol. Macromol. 60 (2013) 272–276.
[32] S.B. Turturro, et al., The effects of cross-linked thermo-responsive PNIPAAm-based hydrogel injection on retinal function, Biomaterials 32 (14) (2011) 3620–3626.
[33] M.J. Caicco, et al., Characterization of hyaluronan-methylcellulose hydrogels for

cell delivery to the injured spinal cord, J. Biomed. Mater. Res. A 101 (5) (2013) 1472–1477.
[34] D. Gupta, C.H. Tator, M.S. Shoichet, Fast-gelling injectable blend of hyaluronan and methylcellulose for intrathecal, localized delivery to the injured spinal cord, Biomaterials 27 (11) (2006) 2370–2379.
[35] Y. Wang, et al., Accelerated release of a sparingly soluble drug from an injectable hyaluronan-methylcellulose hydrogel, J. Control. Release 140 (3) (2009) 218–223.
[36] K. Vulic, M.S. Shoichet, Tunable growth factor delivery from injectable hydrogels for tissue engineering, J. Am. Chem. Soc. 134 (2) (2012) 882–885.
[37] K. Vulic, et al., Mathematical model accurately predicts protein release from an affinity-based delivery system, J. Control. Release 197 (2015) 69–77.
[38] M.M. Pakulska, K. Vulic, M.S. Shoichet, Affinity-based release of chondroitinase ABC from a modified methylcellulose hydrogel, J. Control. Release 171 (1) (2013) 11–16.
[39] R.Y. Tam, M.J. Cooke, M.S. Shoichet, A covalently modified hydrogel blend of hyaluronan-methylcellulose with peptides and growth factors influences neural stem/progenitor cell fate, J. Mater. Chem. 22 (37) (2012) 19402–19411.
[40] H.P. Erickson, Size and Shape of Protein Molecules at the Nanometer Level Determined by Sedimentation, Gel Filtration, and Electron Microscopy, Biol. Procedures Online 11 (2009) 32–51.
[41] H. Fam, M. Kontopoulou, J.T. Bryant, Effect of concentration and molecular weight on the rheology of hyaluronic acid/bovine calf serum solutions, Biorheology 46 (1) (2009) 31–43.
[42] F. Yu, et al., Rheological studies of hyaluronan solutions based on the scaling law and constitutive models, Polymer 55 (1) (2014) 295–301.
[43] M.M. Lavail, et al., Protection of mouse photoreceptors by survival factors in retinal degenerations, Invest. Ophthalmol. Vis. Sci. 39 (3) (1998) 592–602.
[44] T.J. McGill, et al., Intraocular CNTF reduces vision in normal rats in a dose-dependent manner, Invest. Ophthalmol. Vis. Sci. 48 (12) (2007) 5756–5766.
[45] J. Tian, et al., Intravitreal infusion: a novel approach for intraocular drug delivery, Sci. Rep. 6 (2016) 37676.
[46] W.Y. Chen, G. Abatangelo, Functions of hyaluronan in wound repair, Wound Repair Regen. 7 (2) (1999) 79–89.
[47] P.N. Bishop, Structural macromolecules and supramolecular organisation of the vitreous gel, Prog. Retin. Eye Res. 19 (3) (2000) 323–344.
[48] D.L. Hugar, A. Ivanisevic, Materials characterization and mechanobiology of the eye, Mater. Sci. Eng. C 33 (4) (2013) 1867–1875.
[49] E. Fouissac, M. Milas, M. Rinaudo, Shear-rate, concentration, molecular weight, and temperature viscosity dependences of hyaluronate, a wormlike polyelectrolyte, Macromolecules 26 (25) (1993) 6945–6951.
[50] Y.J. Chen, et al., Stability and folding of the SH3 domain of Bruton's tyrosine kinase, Proteins 26 (4) (1996) 465–471.
[51] W.A. Lim, R.O. Fox, F.M. Richards, Stability and peptide binding affinity of an SH3 domain from the Caenorhabditis elegans signaling protein Sem-5, Protein Sci. A Publ. Protein Soc. 3 (8) (1994) 1261–1266.
[52] J. Parker, N. Mitrousis, M.S. Shoichet, Hydrogel for simultaneous tunable growth factor delivery and enhanced viability of encapsulated cells in vitro, Biomacromolecules 17 (2) (2016) 476–484.
[53] Y. Li, et al., CNTF induces regeneration of cone outer segments in a rat model of retinal degeneration, PLoS One 5 (3) (2010) e9495.
[54] R. Wen, et al., Regulation of rod phototransduction machinery by ciliary neurotrophic factor, J. Neurosci. 26 (52) (2006) 13523–13530.
[55] L. Calderone, et al., Acute reversible cataract induced by xylazine and by ketamine-xylazine anesthesia in rats and mice, Exp. Eye Res. 42 (4) (1986) 331–337.
[56] P.V. Turner, et al., Susceptibility of rats to corneal lesions after injectable anesthesia, Comp. Med. 55 (2) (2005) 175–182.
[57] M.A. Bermudez, et al., Time course of cold cataract development in anesthetized mice, Curr. Eye Res. 36 (3) (2011) 278–284.
[58] A.M. Timmers, et al., Subretinal injections in rodent eyes: effects on electrophysiology and histology of rat retina, Mol. Vision 7 (2001) 131–137.
[59] S.D. Varma, et al., Oxidative stress on lens and cataract formation: role of light and oxygen, Curr. Eye Res. 3 (1) (1984) 35–57.
[60] C.J. Zeiss, et al., CNTF induces dose-dependent alterations in retinal morphology in normal and rcd-1 canine retina, Exp. Eye Res. 82 (3) (2006) 395–404.
[61] K.D. Rhee, et al., CNTF-mediated protection of photoreceptors requires initial activation of the cytokine receptor gp130 in Muller glial cells, Proc. Natl. Acad. Sci. U. S. A. 110 (47) (2013) 4.
[62] J.M. Askvig, J.A. Watt, The MAPK and PI3K pathways mediate CNTF-induced neuronal survival and process outgrowth in hypothalamic organotypic cultures, J. Cell Commun. Signal. 9 (3) (2015) 217–231.
[63] K.D. Rhee, et al., Molecular and cellular alterations induced by sustained expression of ciliary neurotrophic factor in a mouse model of retinitis pigmentosa, Invest. Ophthalmol. Vis. Sci. 48 (3) (2007) 1389–1400.
[64] K.J. Wahlin, et al., Neurotrophic factors cause activation of intracellular signaling pathways in Muller cells and other cells of the inner retina, but not photoreceptors, Invest. Ophthalmol. Vis. Sci. 41 (3) (2000) 927–936.
[65] B.G. Ballios, et al., A hydrogel-based stem cell delivery system to treat retinal degenerative diseases, Biomaterials 31 (9) (2010) 2555–2564.
[66] M. Cayouette, C. Gravel, Adenovirus-mediated gene transfer of ciliary neurotrophic factor can prevent photoreceptor degeneration in the retinal degeneration (rd) mouse, Hum. Gene Ther. 8 (4) (1997) 423–430.
[67] B. Chang, et al., Retinal degeneration mutants in the mouse, Vis. Res. 42 (4) (2002) 517–525.
[68] M.M. Pakulska, C.H. Tator, M.S. Shoichet, Local delivery of chondroitinase ABC with or without stromal cell-derived factor 1alpha promotes functional repair in the injured rat spinal cord, Biomaterials 134 (2017) 13–21.
[69] M. Cayouette, et al., Pigment epithelium-derived factor delays the death of photoreceptors in mouse models of inherited retinal degenerations, Neurobiol. Dis. 6 (6) (1999) 523–532.
[70] T. Leveillard, et al., Identification and characterization of rod-derived cone viability factor, Nat. Genet. 36 (7) (2004) 755–759.
[71] J. Tombran-Tink, C.J. Barnstable, PEDF: a multifaceted neurotrophic factor, Nat. Rev. Neurosci. 4 (8) (2003) 628–636.
[72] Y. Yang, et al., Functional cone rescue by RdCVF protein in a dominant model of retinitis pigmentosa, Mol. Ther. 17 (5) (2009) 787–795.